Research Article

Ocular Oncology and Pathology

Ocul Oncol Pathol 2019;5:369–378
DOI: 10.1159/000495841

Received: January 9, 2018
Accepted after revision: November 23, 2018
Published online: February 7, 2019

Choroidal Nevus with Retinal Invasion in 8 Cases

Stephanie J. Weiss[a, b] Christina Stathopoulos[a, c] Carol L. Shields[a]

[a]Ocular Oncology Service, Wills Eye Hospital, Thomas Jefferson University, Philadelphia, PA, USA;
[b]Retina Service, Department of Ophthalmology, Weill Cornell Medical College, New York, NY, USA;
[c]Jules-Gonin Eye Hospital, Fondation Asile des Aveugles, University of Lausanne, Lausanne, Switzerland

Keywords
Choroid · Melanocytoma · Melanoma · Nevus · Retinal invasion

Abstract
Purpose: Choroidal nevus can cause overlying chronic retinal pigment epithelium (RPE) degenerative features, but frank retinal invasion is exquisitely rare. ***Procedures:*** This is a retrospective review of 8 cases of choroidal nevus with retinal invasion with evaluation of clinical and imaging features. ***Results:*** At the time of diagnosis of choroidal nevus with retinal invasion, mean patient age was 65 years. Mean tumor basal diameter was 7 mm, and mean thickness was 2.3 mm. Retinal invasion was ophthalmoscopically visible in all eyes. Related features included drusen (n = 4/8) and RPE fibrous metaplasia (n = 2/8). Overlying lipofuscin, subretinal fluid, RPE detachment, and retinal edema were absent. On B-scan ultrasonography, the lesion was dome-shaped (n = 7/7) and echo-dense (n = 6/7). Optical coherence tomography demonstrated outer retinal invasion (n = 8/8) with additional inner retinal invasion (n = 3/8). The tissue was hypoautofluorescent at the site of invasion (n = 6/7). Over a mean follow-up of 40 months, tumor enlargement was detected in 2 eyes and managed with observation (<1 mm enlargement) or plaque radiotherapy (5 mm enlargement). Nevus hypoautofluorescence was correlated with nevus stability (p = 0.035). ***Conclusion:*** Retinal invasion of the choroidal nevus is rare. In this series of 8 cases, only 1 demonstrated transformation to melanoma over a mean interval of 40 months. Long-term monitoring of such lesions is warranted.

Introduction

Choroidal nevus is a fairly common intraocular tumor, found predominantly in Caucasians, with a prevalence of 4.7% in the US adult population and 6.5% in the Australian population [1, 2]. Qiu and Shields [1] provided a cross-sectional analysis of the prevalence of choroidal nevus using the National Health and Nutrition Examination Survey and found a prevalence of 5.6% in whites, 2.7% in Hispanics, and 0.6% in blacks. This same study documented nevus prevalence to increase with age, as the prevalence was 4.7% in subjects aged 40–49 years, 3.1% in those 50–59 years, 5.4% in those 60–69 years, 6.6% in those 70–79 years, and 7.5% in those >80 years [1].

Choroidal nevus is typically less than 2 or 3 mm in thickness and always located deep to the retinal pigment epithelium (RPE) [3]. Rupture of Bruch membrane/RPE complex with mushroom-shaped tumor growth is a fea-

KARGER

E-Mail karger@karger.com
www.karger.com/oop

Carol L. Shields, MD
Ocular Oncology Service, Suite 1440
Wills Eye Hospital, 840 Walnut Street
Philadelphia, PA 19107 (USA)
E-Mail carolshields@gmail.com

ture of choroidal melanoma but not nevus [3]. Based on clinical features in 3,422 cases of choroidal nevus, common related findings included RPE/Bruch membrane disturbance with overlying drusen (53%), RPE atrophy (11%), RPE fibrous metaplasia (8%), and RPE detachment (1%), but no case of obvious Bruch membrane/RPE rupture [3]. In that analysis, however, choroidal nevus with intraretinal invasion was documented in <1% of patients (6 cases) [3]. A PubMed review of terms including "choroid," "nevus," "retina," and "invasion" yielded 0 publications on this topic.

There has been no previous publication specifically on retinal invasion by choroidal nevus. Retinal invasion has been described with choroidal melanoma and represents a particularly aggressive form of malignancy [4, 5]. Milman et al. [4] described histopathologic features of 4 eyes with retinoinvasive choroidal melanoma, all of which had been previously irradiated. They calculated that 1.4% of irradiated choroidal melanomas demonstrate retinoinvasive features [4]. In this analysis, we specifically focused on the clinical features, multimodal imaging, and outcomes of retinal invasion of choroidal nevus.

Methods

A computerized search for the keywords "choroid nevus" and "retina invasion" from the Ocular Oncology Service, Wills Eye Hospital, Philadelphia, PA, USA, between November 1, 1975, and March 31, 2017, was conducted. Identified charts were retrospectively reviewed. Institutional review board approval was obtained from Wills Eye Hospital.

The charts were reviewed for demographic, clinical, and imaging features at diagnosis, and follow-up outcomes were assessed. The patient demographic data included age at time of diagnosis, sex, and race. Clinical data in the affected eye included Snellen best corrected visual acuity, lens status, and tumor features, including quadrantic localization of tumor epicenter, degree of pigmentation (amelanotic/melanotic), basal diameter (mm), thickness (mm), and related overlying features, such as drusen, orange pigment, RPE alterations (hyperplasia, atrophy, and fibrous metaplasia), subretinal fluid (SRF), and subretinal hemorrhage.

B-scan ultrasonography data (EyeCubed I3, Ellex Innovative Imaging, Sacramento, CA, USA; VuMax HD, Sonomed Escalon, New Hyde Park, NY, USA) were used to image each lesion for tumor thickness (mm), configuration (dome-shaped/mushroom/flat), and density (hollow/solid). Optical coherence tomography (OCT) (Heidelberg Spectralis, Heidelberg Engineering Inc., Vista, CA, USA; Avanti, Optovue, Inc., Fremont, CA, USA; Cirrus HD-OCT, Carl Zeiss Meditec, Inc., Dublin, CA, USA; and Stratus OCT, Carl Zeiss Meditec, Inc.) was used to study the presence of drusen, SRF, overlying RPE alterations, retinal edema, and features of retinal invasion. Autofluorescence imaging (Topcon TRC-50DX Retinal Camera, Topcon America, Paramus, NJ, USA; excitation light bandwidth 535–585 nm and barrier filter bandwidth 605–715 nm) included presence of hypo-, iso-, or hyperautofluorescence overlying the nevus.

Fluorescein angiography data (Topcon TRC-50DX Retinal Camera) were used to evaluate the status of the overlying RPE. OCT-angiography (Cirrus OCT, Carl Zeiss Meditec, Inc.) was performed to study overlying tissue for vasculature characteristics at the nevus site.

Clinical follow-up data included visual acuity, tumor growth, development of new SRF and orange pigment, vitreous seeds, and malignant transformation into melanoma.

Statistical Analysis

All data were tabulated using Microsoft Excel 2011. Unpaired Student's *t* test was used for evaluation of differences in continuous data and Fisher's exact test for categorical data. All statistics were calculated using SPSS, version 17.0 (SPSS Inc., Chicago, IL, USA), and statistical significance was defined as $p < 0.05$.

Case Reports

Case 1

An asymptomatic 71-year-old male presented with best corrected Snellen visual acuity of 20/25 in the left eye (OS). Anterior segment examination was unremarkable. Funduscopic examination was significant for a pigmented choroidal nevus located in the inferior periphery measuring 6.5 mm in the greatest basal diameter (Fig. 1a). An area of retinal invasion was clinically evident as a deeply pigmented central portion of the nevus. There were associated drusen. Overlying orange pigment and SRF were absent. OCT confirmed the presence of a choroidal mass invading through a break in Bruch membrane with inner retinal invasion (Fig. 1f). B-scan ultrasonography revealed a dome-shaped optically dense lesion measuring 2.7 mm in thickness (Fig. 1b). At this time, observation was elected.

Case 2

An asymptomatic 68-year-old male presented with best corrected Snellen visual acuity of 20/40 OS. Anterior segment examination was unremarkable. Funduscopic examination was significant for a nonpigmented choroidal nevus located juxtapapillary measuring 5.5 mm in the greatest basal diameter (Fig. 2a). An area of retinal invasion was clinically evident as a protruding amelanotic choroidal mass near the central portion of the nevus. Overlying orange pigment and SRF were absent. OCT confirmed the presence of a choroidal mass invading through a break in Bruch membrane with inner retinal invasion (Fig. 2b). B-scan ultrasonography revealed a dome-shaped optically dense lesion measuring 2.6 mm in thickness. At this time, observation was elected. Upon follow-up 95 months later, the choroidal nevus remained stable without growth or development of malignant features.

Case 3

An asymptomatic 62-year-old male presented with best corrected Snellen visual acuity of 20/20 in the right eye (OD). Anterior segment examination was unremarkable. Funduscopic examination was significant for a pigmented choroidal nevus located in the superonasal periphery measuring 10 mm in the greatest basal diameter (Fig. 2c). An area of retinal invasion was clinically evident

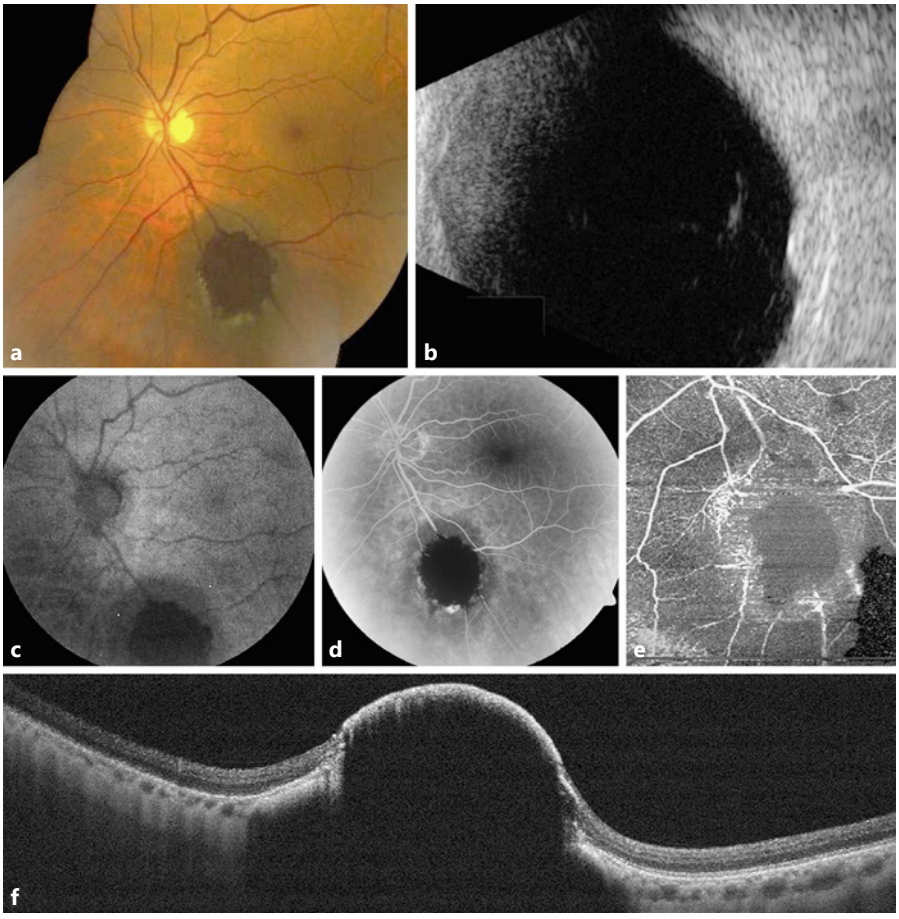

Color version available online

Fig. 1. A 71-year-old male with choroidal nevus demonstrating retinal invasion. Case 1: **a** The pigmented choroidal tumor showed marked dark central pigmentation within the retina, hiding the retinal vessels and surrounded by trace exudation. **b** B-scan ultrasonography documented a dome-shaped, dense choroidal mass with a thickness of 2.7 mm. **c** Autofluorescence depicted central hypoautofluorescence at the site of the invasion. Fluorescein angiography (**d**) and optical coherence tomography angiography (**e**) showed central blocked perfusion corresponding to the area of invasion. **f** Enhanced depth imaging-optical coherence tomography through the nevus showed central invasion of the retina.

as a deeply pigmented central portion of the nevus. There were associated fibrous metaplasia and drusen. Overlying orange pigment and SRF were absent.

OCT confirmed the presence of a choroidal mass invading through a break in Bruch membrane with inner retinal invasion (Fig. 2d). B-scan ultrasonography revealed a dome-shaped optically dense lesion measuring 2.8 mm in thickness. At this time, observation was elected. Despite a limited follow-up period, the choroidal nevus remained stable without growth or development of malignant features upon follow-up 3 months later.

Case 4

An asymptomatic 62-year-old female presented with best corrected Snellen visual acuity of 20/25 OD. Anterior segment examination was unremarkable. Funduscopic examination was significant for a pigmented choroidal nevus located in the superior periphery measuring 5 mm in the greatest basal diameter and 1.6 mm in thickness (Fig. 2e). An area of retinal invasion was clinically evident as a deeply pigmented central portion of the nevus. There were associated drusen. Overlying orange pigment and SRF were absent. OCT confirmed the presence of a choroidal mass invading through a break in Bruch membrane with outer retinal invasion (Fig. 2f). At this time, observation was elected. Upon follow-up 30 months later, the choroidal nevus remained stable without growth or development of malignant features.

Case 5

An asymptomatic 84-year-old female presented with best corrected Snellen visual acuity of 20/25 OS. Anterior segment examination was unremarkable. Funduscopic examination was significant for a pigmented choroidal nevus located in the inferior periphery measuring 9 mm in the greatest basal diameter (Fig. 2g). An area of retinal invasion was clinically evident as a deeply pigmented central portion of the nevus. There were associated drusen. Overlying orange pigment and SRF were absent. OCT confirmed the presence of a choroidal mass invading through a break in Bruch membrane with outer retinal invasion (Fig. 2h). B-scan ultrasonography revealed a dome-shaped optically dense lesion measuring 2.1 mm in thickness. At this time, observation was elected. Upon follow-up 18 months later, the choroidal nevus remained stable without growth or development of malignant features.

Case 6

An asymptomatic 31-year-old male presented with best corrected Snellen visual acuity of 20/30 OS. Anterior segment examination was unremarkable. Funduscopic examination was significant for a pigmented choroidal nevus located in the temporal periphery measuring 9 mm in the greatest basal diameter (Fig. 2i). An area of retinal invasion was clinically evident as a deeply pigmented central portion of the nevus. There was associated fibrous metaplasia.

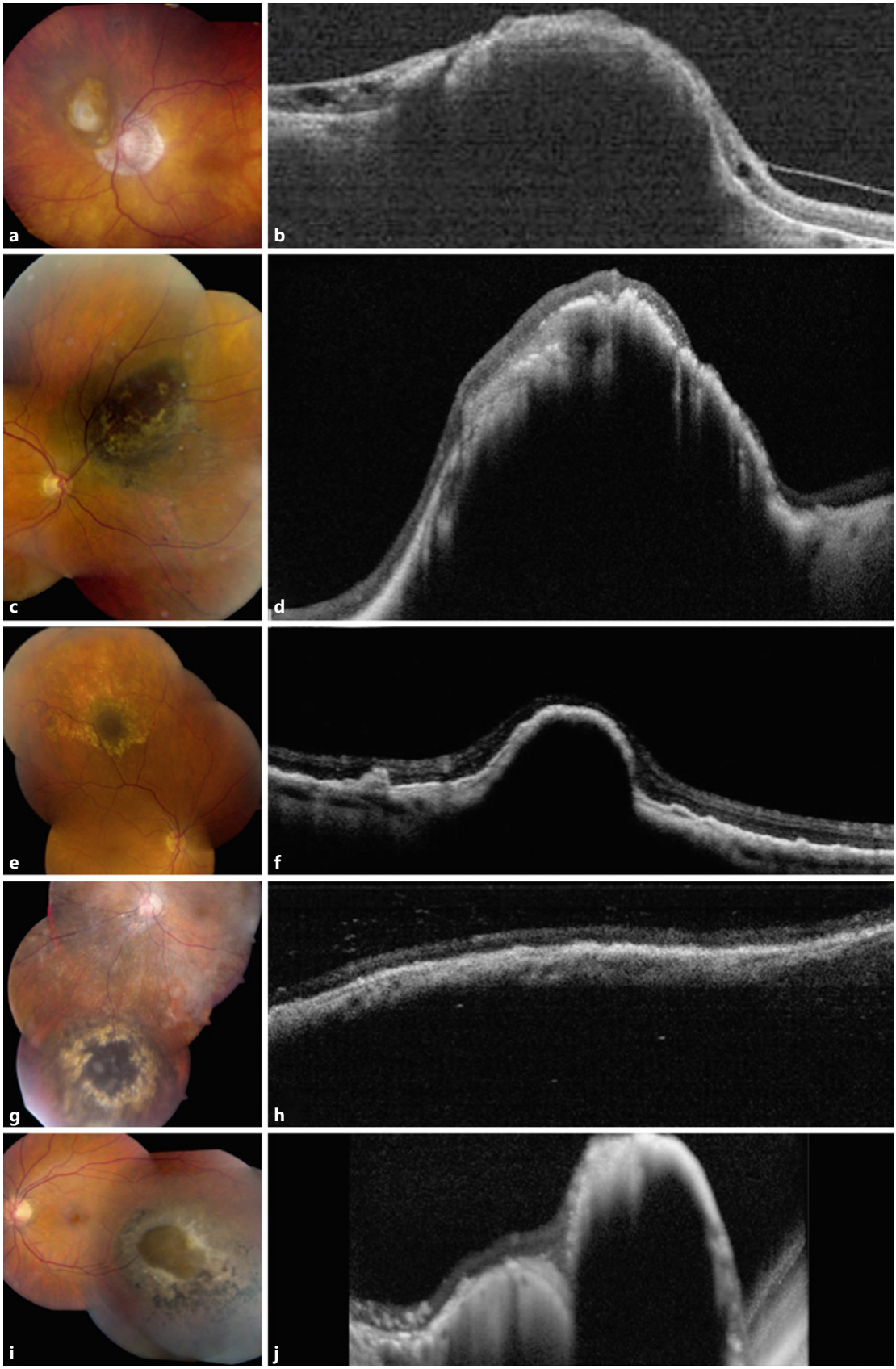

Color version available online

2

(For legend see next page.)

Overlying orange pigment and SRF were absent. OCT confirmed the presence of a choroidal mass invading through a break in Bruch membrane with outer retinal invasion (Fig. 2j). B-scan ultrasonography revealed a dome-shaped optically dense lesion measuring 3.3 mm in thickness. At this time, observation was elected.

Case 7

An asymptomatic 69-year-old female presented with best corrected Snellen visual acuity of 20/25 OD. Anterior segment examination was unremarkable. Funduscopic examination was significant for a pigmented choroidal nevus located in the temporal periphery measuring 4 mm in the greatest basal diameter (Fig. 3a). An area of retinal invasion was clinically evident as a deeply pigmented central portion of the nevus. There was associated fibrous metaplasia.

Overlying orange pigment and SRF were absent. OCT confirmed the presence of a choroidal mass invading through a break in Bruch membrane with outer retinal invasion (Fig. 3c). B-scan ultrasonography revealed a dome-shaped optically dense lesion measuring 2.2 mm in thickness. At this time, observation was elected. Upon follow-up 24 months later, the choroidal lesion demonstrated an increase of 5 mm in basal diameter and 0.3 mm in thickness with development of overlying orange pigment (Fig. 3d). At this time, the lesion was treated for malignant transformation to choroidal melanoma with an Iodine-125 (I-125) ra-

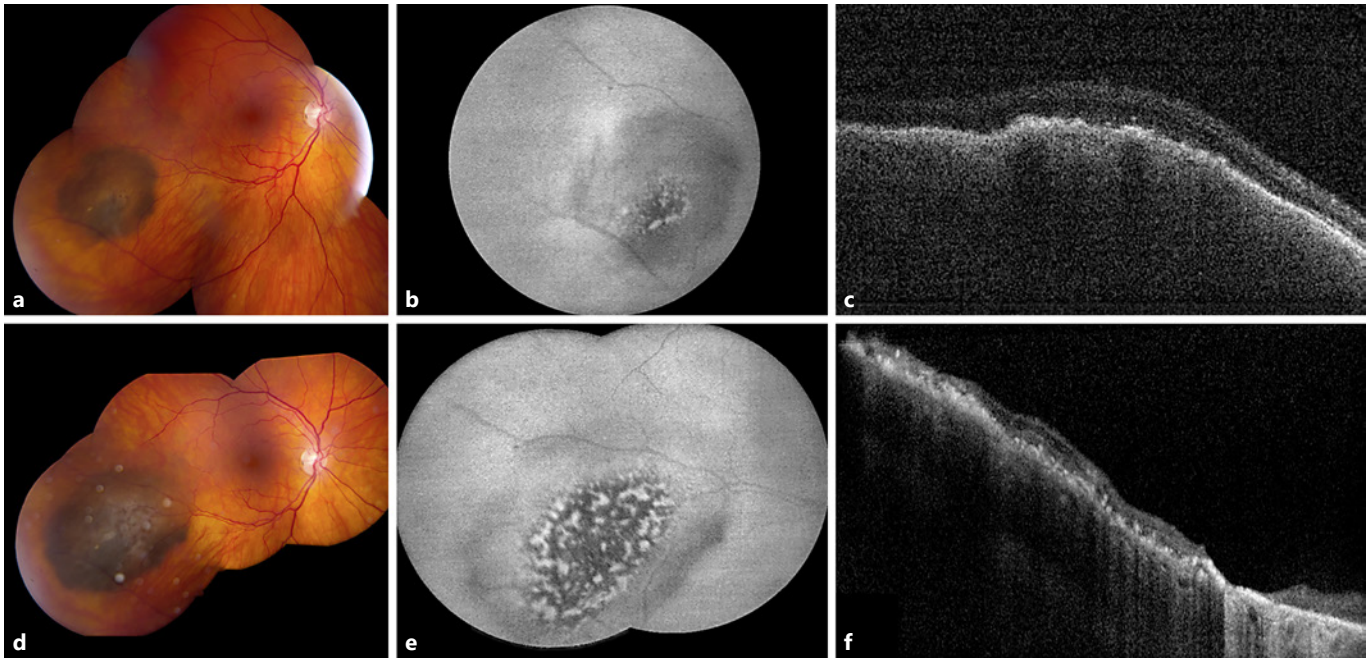

Color version available online

Fig. 3. Choroidal nevus with retinal invasion demonstrating transformation to melanoma. Case 7: on presentation, the pigmented choroidal lesion showed a central area of increased pigmentation obscuring the retinal vessels (**a**) with outer retinal invasion evident on OCT (**c**). While overlying fibrous metaplasia was present, orange pigment and subretinal fluid were not present. **b** Autofluorescence showed hypoautofluorescence of the lesion with small central areas of hyperautofluorescence. **d** On follow-up 24 months later, the choroidal tumor demonstrated growth in basal dimension by 5 mm. Subretinal fluid was not present. **e** Autofluorescence showed increased areas of hyperautofluorescence of the lesion representing the presence of lipofuscin. These findings were consistent with transformation to melanoma. **f** Following plaque radiotherapy, regression of the tumor and subsequent retinal atrophy were noted.

Fig. 2. Optical coherence tomography (OCT) of choroidal nevus with retinal invasion. Case 2: clinical appearance (**a**) and OCT (**b**) of a juxtapapillary choroidal nevus with overlying fibrous metaplasia of the retinal pigment epithelium (RPE) demonstrating overlying retinal invasion and thinning. These features remained stable at 95 months' follow-up. Case 3: clinical appearance (**c**) and OCT (**d**) of a superonasal choroidal nevus with overlying patchy fibrous metaplasia of the RPE showing dark central invasion, confirmed on OCT with extreme retinal thinning and disorganization. Despite a limited follow-up period, these findings were stable 3 months later. Case 4: clinical appearance (**e**) and OCT (**f**) of a superior choroidal nevus surrounded by drusen and capped by a dark appearance representing invasion with thinning of the RPE and retina. These findings were stable at 30 months' follow-up. Case 5: clinical appearance (**g**) and OCT (**h**) of an inferior choroidal nevus with overlying fibrous metaplasia of the RPE. These findings were stable at 18 months' follow-up. Case 6: clinical appearance (**i**) and OCT (**j**) of an inferotemporal choroidal nevus with a central break of Bruch membrane and retinal invasion surrounded by RPE alterations.

Table 1. Choroidal nevus with retinal invasion in 8 patients; demographics

	Total (n = 8 eyes)	Stable nevus (n = 6 eyes)	Growth of nevus (n = 2 eyes)	p value*
Mean age (median; range), years	65 (69; 31–84)	63 (65; 31–84)	70 (70; 69–71)	0.613
Gender, n (%)				0.429
Male	4 (50)	4 (67)	0 (0)	
Female	4 (50)	2 (33)	2 (100)	
Race, n (%)				1.00
Caucasian	7 (88)	5 (83)	2 (100)	
Hispanic	1 (12)	1 (17)	0 (0)	

* Fisher's exact test.

dioactive plaque. Following plaque radiotherapy, regression of the tumor was noted. The regressed choroidal melanoma remained stable upon the most recent follow-up 22 months after treatment.

Case 8

An asymptomatic 71-year-old female presented with best corrected Snellen visual acuity of 20/20 OS. Anterior segment examination was unremarkable. Funduscopic examination was significant for a pigmented choroidal nevus located in the inferior periphery measuring 5 mm in the greatest basal diameter. An area of retinal invasion was clinically evident as a deeply pigmented central portion of the nevus. Overlying orange pigment and SRF were absent. OCT confirmed the presence of a choroidal mass invading through a break in Bruch membrane with outer retinal invasion. B-scan ultrasonography revealed a dome-shaped optically dense lesion measuring 1.4 mm in thickness. At this time, observation was elected. Upon follow-up 12 months later, the choroidal nevus demonstrated minimal growth with an increase of 0.5 mm in thickness. The remainder of the nevus remained stable without evidence of orange pigment or SRF. Observation was once again elected, and the lesion remained stable without growth or development of malignant features upon follow-up 50 months after initial presentation.

Results

There were 8 eyes of 8 patients with retinal invasion from choroidal nevus included in this study. The demographic features are summarized in Table 1. The mean age at diagnosis was 65 years (median 69 years, range 31–84 years).

The clinical features are listed in Table 2. The visual acuity was 20/40 or better in all cases (8/8). The retinal invasion was clinically evident in all 8 patients (Fig. 1a, 2a, c, e, g, i). The mean distance from the tumor to the optic disc was 5 mm (median 6 mm, range 0–9 mm), and to the foveola, it was 5 mm (median 4 mm, range 3–11 mm). The mean largest basal diameter was 7 mm (median 6 mm, range 4–10 mm), and the mean thickness was 2.3 mm (median 2.4 mm, range 1.4–3.3 mm). Orange pigment and SRF were not present in any case.

The imaging characteristics are provided in Table 3. Ultrasonography revealed a dome-shaped configuration (7/7) and was acoustically dense (6/7) (Fig. 1b) or hollow (1/7). OCT over the nevus documented rupture of Bruch membrane with outer retinal invasion (8/8) and with additional inner retinal invasion (3/8) (Fig. 2b, d, f, h, j). By OCT, related features included drusen (1/8), RPE hyperplasia (2/8), RPE atrophy (2/8), RPE fibrous metaplasia (2/8), and subclinical subretinal cleft (1/8). Choroidal neovascularization was not present in any case. The nevus demonstrated hypoautofluorescence (Fig. 1c) (6/7) and mixed hyper- and hypoautofluorescence (1/7). Fluorescein angiography, performed in 1 patient, revealed hypofluorescence of the nevus with retinal nonperfusion at the site of invasion (Fig. 1d). OCT-angiography, performed in 1 patient, documented retinal vasculature absence in the area corresponding to the retinal invasion (Fig. 1e).

The outcomes are presented in Table 4. Over a mean follow-up of 40 months (median 38 months, range 3–95 months), the nevus remained stable (6/8) or with <1 mm enlargement (1/8). There was 1 case that demonstrated progressive development of overlying lipofuscin seen clinically and on autofluorescence and 5 mm enlargement in basal diameter, classified as growth into melanoma (Fig. 3a–f). This patient was treated with I-125 plaque radiotherapy and later developed radiation maculopathy and vision loss. The remainder of eyes showed stable visual acuity.

A comparison of the stable (6/8) with enlarging (2/8) nevi revealed no significant differences in demographic or clinical data (Tables 1, 2), but there was a difference in autofluorescence with a low signal in those patients that remained stable (p = 0.035) (Table 3).

Table 2. Choroidal nevus with retinal invasion in 8 patients; clinical features at initial evaluation

	Total (n = 8 eyes)	Stable nevus (n = 6 eyes)	Growth of nevus (n = 2 eyes)	p value*
Eye				1.00
Right	3 (37)	2 (33)	1 (50)	
Left	5 (63)	4 (67)	1 (50)	
Best corrected visual acuity (Snellen)				
Mean	20/25	20/25	20/25	0.349†
Median	20/25	20/25	20/25	
20/40 or better	8 (100)	6 (100)	2 (100)	1.00
20/50 or worse	0 (0)	0 (0)	0 (0)	
Ocular melanocytosis	3 (37)	2 (33)	1 (50)	1.00
Lens status				
Clear	1 (12)	1 (17)	0 (0)	1.00
Cataract	5 (63)	4 (67)	1 (50)	1.00
Intraocular lens	2 (25)	1 (17)	1 (50)	1.00
Nevus meridian				
Superior	1 (12)	1 (17)	0 (0)	1.00
Temporal	2 (25)	1 (17)	1 (50)	0.463
Inferior	3 (38)	2 (33)	1 (50)	1.00
Nasal	2 (25)	2 (33)	0 (0)	1.00
Anterior margin of nevus				1.00
Macula	3 (37)	2 (33)	1 (50)	
Macula to equator	5 (63)	4 (67)	1 (50)	
Posterior margin of nevus				
Macula	1 (12)	0 (0)	1 (50)	0.250
Macula to equator	6 (75)	5 (83)	1 (50)	0.463
Equator to ora serrata	1 (12)	1 (17)	0 (0)	1.00
Mean distance to optic nerve (median; range), mm	5 (6; 0–9)	5 (5; 0–9)	6 (6; 5–8)	0.494†
Mean distance to fovea (median; range), mm	5 (4; 3–11)	5 (4; 3–11)	4 (4; 3–5)	0.640†
Mean largest diameter (median; range), mm	7 (6; 4–10)	7.5 (7.8, 5–10)	4.5 (4.5; 4–5)	0.106†
Mean thickness (median; range), mm	2.3 (2.4; 1.4–3.3)	2.5 (2.7; 1.6–3.3)	1.8 (1.8; 1.4–2.2)	0.185†
Bruch membrane rupture	8 (100)	6 (100)	2 (100)	1.00
Retinal invasion	8 (100)	6 (100)	2 (100)	1.00
Drusen	4 (50)	4 (67)	0 (0)	0.429
Orange pigment	0 (0)	0 (0)	0 (0)	1.00
Subretinal hemorrhage	1 (12)	1 (17)	0 (0)	1.00
Subretinal fluid	0 (0)	0 (0)	0 (0)	1.00
Fibrous metaplasia of overlying retinal pigment epithelium	2 (25)	2 (33)	0 (0)	1.00

Values are n (%) unless otherwise indicated. * Fisher's exact test. † Student's t test.

Discussion

Retinal invasion from underlying choroidal nevus is rare. This finding typically clinically appears with dense intraretinal and choroidal pigmentation at the site of a pigmented nevus, retinal angiographic blocked perfusion at the site, and OCT evidence of tumor growth through Bruch membrane with entry as optically dense material into the outer retina. The pigmentation carries a brown hue from the choroidal mass and not a black hue found with RPE hyperplasia. In cases of amelanotic nevi, the site of nevus invasion appears as an amelanotic choroidal mass without the overlying black hue of RPE hyperplasia. The degree of retinal blocked perfusion depends on the extent of retinal invasion. This angiographic feature is similar to that found with choroidal melanoma demon-

Table 3. Choroidal nevus with retinal invasion in 8 patients; imaging findings at initial examination

	Total (n = 8 eyes)	Stable nevus (n = 6 eyes)	Growth of nevus (n = 2 eyes)	p value*
Ultrasound features (n = 7)				
Configuration				
Dome	7 (100)	5 (100)	2 (100)	1.00
Density				
Hollow	1 (14)	1 (17)	0 (0)	1.00
Dense	6 (86)	4 (67)	2 (100)	1.00
Optical coherence tomography features (n = 8)				
Depth of invasion				
Bruch membrane rupture with outer retinal invasion	5 (63)	3 (50)	2 (100)	0.464
Bruch membrane rupture with outer and inner retinal invasion	3 (37)	3 (50)	0 (0)	0.464
Drusen	1 (12)	1 (17)	0 (0)	1.00
Subretinal fluid	1 (12)	1 (17)	0 (0)	1.00
Intraretinal edema	0 (0)	0 (0)	0 (0)	1.00
RPE atrophy	2 (25)	1 (17)	1 (50)	0.463
RPE hyperplasia	2 (25)	2 (33)	0 (0)	1.00
RPE fibrous metaplasia	2 (25)	2 (33)	0 (0)	1.00
Choroidal neovascularization	0 (0)	0 (0)	0 (0)	1.00
Fundus autofluorescence features (n = 7)				
Hyperautofluorescence	0 (0)	0 (0)	0 (0)	1.00
Hypoautofluorescence	6 (86)	6 (100)	0 (0)	*0.035*
Mixed hyper- and Hypoautofluorescence	1 (14)	0 (0)	1 (100)	0.143
Fluorescein angiography features (n = 1)				
Hypofluorescence	1 (100)	1 (100)	na	–

Values are n (%). na, not applicable. Italics indicate statistical significance. * Fisher's exact test.

strating retinal invasion [6]. Upon comparison of previously reported choroidal nevus data [3] with this cohort of nevus invasion into the retina, we found that the mean tumor base and thickness were larger in these cases with retinal invasion (vs. nevus in general) (6.8 vs. 4.9 mm in base and 2.3 vs. 1.5 mm in thickness).

Over the past decade, OCT has been helpful in the documentation of retinal microanatomical changes overlying choroidal nevus [3, 7, 8]. In an evaluation of 120 eyes with choroidal nevus studied by OCT, photoreceptor loss or thinning was present in 61 (51%), retinal disorganization in 51 (42%), retinal thinning in 26 (22%), retinal edema in 18 (15%), SRF in 26 (22%), and RPE detachment in 15 (13%) [7]. It was suggested that some of the outer retinal alterations could be caused by a compressive effect of the nevus on the choriocapillaris leading to outer retinal ischemia [9]. Espinoza et al. [8] studied OCT patterns over choroidal nevus to characterize retinal changes and found 3 types, including a "negative OCT pattern" with no retinal changes, an "active OCT pattern" with localized SRF and serous retinal detachment indicating a higher likelihood of potential growth, and a "chronic OCT pattern" with atrophic retinal changes including overlying retinal thinning and RPE metaplasia indicating a likelihood of long-term stability. In our series, OCT demonstrated Bruch membrane disruption in all cases, outer retinal invasion involving the RPE and photoreceptor layer in 5 cases, and deeper invasion to inner retinal layers (Fig. 1f) in 3 cases.

The mechanism by which choroidal nevus invades the retina is unclear. Shields et al. [3] analyzed 3,422 consecutive eyes with choroidal nevus, presenting at a mean age of 60 years, and correlated increased multiplicity of nevi, nevus thickness, and presence of drusen with increasing age. Drusen represent a chronic overlying degeneration of the RPE and Bruch membrane [3]. In fact, drusen were noted in only 11% of those aged ≤20 years, 40% of those aged 21–50 years, and 58% of those aged >50 years (p < 0.001) [3]. In that large series, there were 6 (<1%) nevi with retinal invasion, all in the age group >50 years (<1%) and none (0%) in those aged ≤20 years or 21–50 years [3]. In the present series, the mean age of patients was 65 years

Table 4. Choroidal nevus with retinal invasion in 8 patients; outcomes

Outcomes	Total (n = 8 eyes)	Stable nevus (n = 6 eyes)	Growth of nevus (n = 2 eyes)	p value*
Follow up, months				
Mean (median; range)	40 (38; 3–95)	37 (24; 3–95)	48 (48; 3–50)	0.724
Growth of lesion	2 (25)	0 (0)	2 (100)	*0.035*
Treatment of growth (n = 2)				
Observation	1 (50)	na	1 (50)	–
Plaque radiotherapy	1 (50)	na	1 (50)	–
Enucleation	0 (0)	na	0 (0)	–
Development of new subretinal fluid	0 (0)	0 (0)	0 (0)	1.00
Development of new orange pigment	1 (12)	0 (0)	1 (50)	0.250
Development of mushroom-shaped configuration	0 (0)	0 (0)	0 (0)	1.00
Development of vitreous seeds	0 (0)	0 (0)	0 (0)	1.00
Transformation from nevus to melanoma	1 (12)	0 (0)	1 (50)	0.250
Treatment of melanoma (n = 1)				
Plaque radiotherapy	1 (100)	na	1 (100)	–
Proton beam radiation	0 (0)	na	0 (0)	–
Enucleation	0 (0)	na	0 (0)	–
Development of metastasis	0 (0)	0 (0)	0 (0)	1.00
Vision loss >3 lines	1 (12)	0 (0)	1 (50)	0.250
Vision 20/200 or worse	0 (0)	0 (0)	0 (0)	1.00
Final visual acuity (n = 6)				
Improved	1 (17)	1 (25)	0 (0)	1.00
Stable	3 (50)	3 (75)	0 (0)	0.463
Worsened	2 (33)	0 (0)	2 (100)	*0.035*

Values are n (%) unless otherwise indicated. na, not applicable. Italics indicate statistical significance. * Fisher's exact test.

(median 69 years), and the youngest patient was 31 years. The older age in this cohort and the presence of features such as drusen (50%), RPE fibrous metaplasia (25%), and Bruch membrane disruption by OCT (100%) suggest that retinal invasion is likely a chronic feature of an inherently weak overlying Bruch membrane that enables nevus invasion. Fundus examination failed to show other signs of Bruch membrane weakness, such as lacquer cracks or angioid streaks, and no patient demonstrated features of myopia.

By OCT imaging, each nevus in this series occupied the entire thickness of the choroid. There were numerous OCT findings of chronicity including drusen (12%), SRF (12%), RPE atrophy (25%), hyperplasia (25%), and fibrous metaplasia (25%). Autofluorescence indicating RPE dysfunction or blocked fluorescence as hypoautofluorescence overlying the nevus was found in 86% and mixed hyper- and hypoautofluorescence in 14%. It should be noted that retinal invasion is not always a benign degenerative finding. There is a type of retinoinvasive melanoma, a particularly aggressive tumor, described as spindle or epithelioid cell type that can invade along the retinal vasculature and optic nerve, often resulting in enucleation [4, 5].

In summary, retinal invasion from choroidal nevus is rare. The mechanism behind invasion could be related to overlying chronic RPE-Bruch membrane degeneration. Definitive conclusions regarding the mechanism of invasion are limited by the absence of histopathology in all 8 cases, which also prevents diagnostic certainty. While it is difficult to establish risk factors for transformation to melanoma given the rarity of this clinical entity and limited sample size in the present study, in only 1 case was transformation into melanoma documented, and there were no clinical features predictive of transformation, except for overlying hyper- and hypoautofluorescence (p = 0.035). Cases of choroidal nevus with evidence of retinal invasion should be monitored closely for evidence of malignant transformation, as retinal invasion is an uncommon feature of choroidal nevus but a relatively common occurrence in cases of choroidal melanoma.

Statement of Ethics

Institutional review board approval for this study was obtained from Wills Eye Hospital.

Disclosure Statement

All authors have no proprietary interests. The authors have no additional financial interests or conflicts of interest to disclose.

Funding Sources

Financial support was provided by the Eye Tumor Research Foundation, Philadelphia, PA, USA (C.L.S.). The founders had no role in the design and conduct of the study, in the collection, analysis, and interpretation of the data, and in the preparation, review, or approval of the manuscript. C.L.S., MD, has had full access to all the data in the study and takes responsibility for the integrity of the data and the accuracy of the data analysis.

References

1 Qiu M, Shields CL. Choroidal Nevus in the United States Adult Population: Racial Disparities and Associated Factors in the National Health and Nutrition Examination Survey. Ophthalmology. 2015 Oct;122(10):2071–83.

2 Sumich P, Mitchell P, Wang JJ. Choroidal nevi in a white population: the Blue Mountains Eye Study. Arch Ophthalmol. 1998 May;116(5):645–50.

3 Shields CL, Furuta M, Mashayekhi A, Berman EL, Zahler JD, Hoberman DM, et al. Clinical spectrum of choroidal nevi based on age at presentation in 3422 consecutive eyes. Ophthalmology. 2008 Mar;115(3):546–552.e2.

4 Milman T, Hu DN, McCormick SA, Eagle RC Jr, Crawford JB, Chin K, et al. Expression of neurotrophin receptors by retinoinvasive uveal melanoma. Melanoma Res. 2012 Apr;22(2):164–8.

5 Kivelä T, Summanen P. Retinoinvasive malignant melanoma of the uvea. Br J Ophthalmol. 1997 Aug;81(8):691–7.

6 Shields JA, Shields CL. Retinal invasion by choroidal melanoma. In: Shields JA, Shields CL. Atlas of Intraocular Tumors. Philadelphia: Lippincott Williams & Wilkins; 1999. pp. 116–7.

7 Shields CL, Mashayekhi A, Materin MA, Luo CK, Marr BP, Demirci H, et al. Optical coherence tomography of choroidal nevus in 120 patients. Retina. 2005 Apr-May;25(3):243–52.

8 Espinoza G, Rosenblatt B, Harbour JW. Optical coherence tomography in the evaluation of retinal changes associated with suspicious choroidal melanocytic tumors. Am J Ophthalmol. 2004 Jan;137(1):90–5.

9 Shah SU, Kaliki S, Shields CL, Ferenczy SR, Harmon SA, Shields JA. Enhanced depth imaging optical coherence tomography of choroidal nevus in 104 cases. Ophthalmology. 2012 May;119(5):1066–72.